

TEMPERATURE DEPENDENCE OF THE RESIDUAL SHEAR STRENGTH: THE ROLE OF CLAY FRACTION

OM PRASAD DHAKAL ¹, MARCO LOCHE ¹, RANJAN KUMAR DAHAL ², GIANVITO SCARINGI ¹

¹ *Institute of Hydrogeology, Engineering Geology and Applied Geophysics, Faculty of Science, Charles University, Prague, Czech Republic; gianvito.scaringi@natur.cuni.cz (corresponding author)*

² *Central Department of Geology, Tribhuvan University Kirtipur, Kathmandu, Nepal*

Abstract

The residual shear strength is a key parameter in slope stability. It can depend on temperature according to the material's composition and hydro-mechanical boundary conditions. However, landslide materials are often heterogeneous and anisotropic, and the role of thermo-mechanical coupling in their behaviour remains poorly understood. We conducted ring-shear experiments on landslide soil samples from the Melamchi catchment in central Nepal, where a large-scale disaster occurred in 2021. We tested water-saturated specimens under normal stresses of 50–150 kPa and a rate of shearing of 0.1 mm/min. After attaining the residual shear condition, we increased the temperature to 50 °C to evaluate a new steady-state value of shear resistance. We explored the role of the clay fraction by progressively removing the coarsest particles according to different cutoff sizes (125, 62, and 20 µm). We observed thermal sensitivity – and, in particular, weakening upon heating – only in specimens with a clay fraction higher than 10%. This finding is consistent with mechanisms of thermal sensitivity observed in fine-grained soils, which are related to physico-chemical interactions in clay minerals.

Keywords

Residual shear strength, temperature, shear rate, landslide, thermo-hydro-mechanical coupling.

1 Introduction

The shear strength is a fundamental parameter governing the stability of soil and rock slopes, as well as the triggering and propagation of landslides. The residual shear strength – a minimum, steady-state value of shearing resistance – is especially relevant in reactivated landslides, where a well-defined shear zone or slip surface has formed and has already undergone large strains or displacements (Skempton, 1964, 1985). In sheared soil or regolith containing clay minerals, the residual shear strength can be significantly lower than the critical state or fully softened shear strength owing to the progressive alignment of clay particles along the direction of shearing. In fact, in face-to-face arrangements, the shearing resistance of water-saturated clay minerals is minimal, and very low values of drained residual friction angle (lower than 5°) can be attained, especially if highly active clays such as smectites are abundant (Mesri and Olson, 1970). Such a low friction angle can promote landslide activity even along gentle slopes and discontinuities (Hu et al., 2018).

The residual shear strength depends on a number of factors, including the normal stress and rate of shearing, the mineral composition, the size and shape of the sheared particles, the chemical composition of the pore fluid, and temperature (Di Maio and Scaringi, 2016; Scaringi et al., 2018; Scaringi and Loche, 2022; Duque et al., 2023; Loche and Scaringi, 2023). Coupled processes of thermo-chemo-hydro-mechanical nature are complex and often lead to counterintuitive responses, such as heating-induced consolidation despite thermal expansion of both water and mineral grains or enhanced hydraulic

conductivity upon exposure to saline solutions despite an important decrease in overall porosity (Mitchell, 1991; Di Maio, 1996). The role of the rate of shearing has been explored extensively in recent years (e.g., Tika et al., 1996; Scaringi et al., 2018; Duque et al., 2023), and significant “rate effects” have been observed for rates above 0.1–1 mm/min (i.e., for strain rates above 10^{-3} – 10^{-1} s $^{-1}$) in usual experimental setups. In the presence of a large proportion of clay minerals, an increase in strength that scales roughly linearly with the logarithm of the rate of shearing is often observed (Scaringi and Di Maio, 2016; Scaringi et al., 2018; Kohler et al., 2023). However, the application of these insights to real-scale problems remains challenging owing to the difficult evaluation of the thickness of the shear zone (and hence the strain rate), its composition, and spatial heterogeneity. Both basal and distributed shearing (internal plastic deformation) can characterise landslide kinematics (Di Maio et al., 2015; Massey et al., 2016).

Few studies have focused on evaluating the effect of temperature on the residual shear strength, and the published results are insufficient for a comprehensive understanding; however, the role of clay minerals has been recognised, and coupling between rate-dependent and temperature-dependent responses has been suggested (Shibasaki et al., 2016, 2017; Garcia et al., 2023; Loche and Scaringi, 2023). More specifically, the largest thermal sensitivity seems to be observed at rates of shearing below the threshold for significant rate effects (0.1–1 mm/min), that is, in a condition of laminar shearing that is likely drained. Notably, very important thermal effects also arise under very large rates of shearing (>0.1 m/s, out of the scope of this work), where frictional heating and, possibly, thermal pressurisation dominate the response (e.g., Goren and Aharonov, 2007).

In the realm of stable or potentially unstable slopes and slow-moving landslides – and in non-freezing conditions – temperature is usually accounted for in models only if slope-vegetation-atmosphere interaction is considered. These models focus on thermo-hydraulic coupling to define the slope hydrology and hydraulics (e.g., water content, infiltration, suction, pore water pressure, seepage) at and near the slope-atmosphere interface (e.g., Guglielmi et al., 2023; Badakhshan et al., 2024). This coupling can affect the stability of a slope by changing the effective stress state while the material’s friction angle remains unaffected. However, in the light of the experimental evidence briefly introduced above, the direct thermo-mechanical coupling can also affect the stability of a slope – and the kinematics of an active landslide – by modifying the frictional resistance of the sheared material (Scaringi and Loche, 2022, 2024). The potential magnitude of this coupling has been quantified numerically (Loche and Scaringi, 2023) and field evidence of slow-moving landslides responding to seasonal changes in temperature has been found (Shibasaki et al., 2016). Climate change may alter the temperature distribution in slopes, particularly in proximity to the surface, where climate extremes and enhanced seasonal excursions may affect slope stability also through thermo-mechanical coupling (Scaringi and Loche, 2022).

In this contribution, we discuss some recent experiments conducted on natural materials sampled from an area that featured widespread landsliding in Nepal. The materials were sheared and exposed to controlled changes in temperature. In the experimental campaign, we focused, in particular, on evaluating the importance of the mineral composition and identifying a threshold clay fraction below which the role of temperature in the residual shear strength can be considered negligible and could be safely excluded from modelling.

2 Materials and methods

2.1 Study area

The Melamchi Valley in central Nepal (**Fig. 1**) experienced a severe flood in 2021 as a result of the propagation of a chain of geohazards. The event was probably initiated by the outburst of a rather small glacial lake (~2500 m-) in the upper reaches of the catchment and amplified by the important runoff

resulting from monsoon rainfall, the entrainment of soil and regolith, and fifteen simultaneously triggered landslides.

Geologically, the Melamchi catchment lies on the southern front of the higher Himalayan sequence that comprises the higher Himalayan crystalline rocks (Dhital, 2015). The catchment extends northwards to the moderately ($35\text{--}45^\circ$) northwest dipping main central thrust that runs in the NW-SE direction. The sequence from the main central thrust is followed by the kyanite-garnet schist of the Talamarang Fm. The overlying Gyalthum Fm. features quartzite mica interlayered by feldspar-garnet-biotite schist. This is followed by a band of Bolde quartzite and finally by the Timbu Fm., where the majority of the landslides took place. The maximum thickness of this formation is 1.1 km and comprises light to dark grey intensely deformed migmatites, banded gneisses, schists, and quartzite. The Timbu Fm. is followed by the overlying Golphu Fm., consisting of dark gray feldspar-garnet-biotite schist, banded gneiss, and laminated quartzite bands.

In the region, the precipitation pattern identifies three seasons: pre-monsoon from January to May, monsoon from June to September, and post-monsoon from October to December. The average annual precipitation for the whole catchment varies from 1200 to 3000 mm, and $\sim 80\%$ of the precipitation occurs during the monsoon season (Shrestha et al., 2016). The average annual temperature ranges from 4 to 33°C . The average annual discharge measured at the Helambu station until 2021 (when the station was swept away) was $\sim 10\text{ m}^3/\text{s}$, with peaks of $\sim 30\text{ m}^3/\text{s}$ during the monsoon season and values as low as $\sim 2.5\text{ m}^3/\text{s}$ during the driest month.

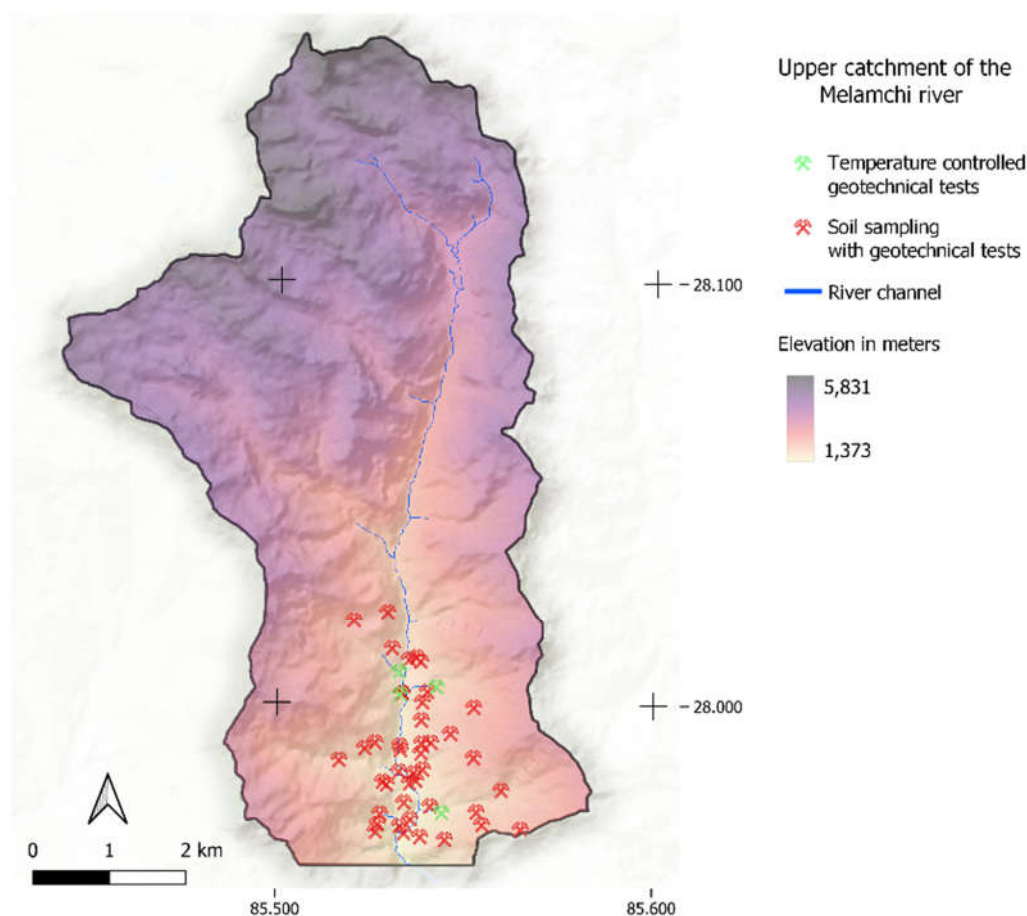


Figure 1. Digital elevation model of the study area with the indication of the sampling sites. Locations marked in green are where the samples for the experiments described in this work were taken.

2.2 Materials

After the 2021 event, an extensive survey was conducted, which included sampling at 70 locations affected by the landslides. Owing to the impossibility of bringing heavy machinery to the sites, sampling was performed using a manual tool and reached depths of ~1 m. We selected four samples for our experimental campaign, which featured different properties and compositions (**Table 1**). The samples were crushed, oven-dried, and sieved, and from each sample, four specimens were obtained by eliminating the coarsest fraction according to different cutoff sizes (125, 62, and 20 μm). Therefore, the specimens submitted to the experiments featured distinct clay fractions (**Table 2**).

Table 1. Basic properties and mineral composition (according to X-ray powder diffraction analysis) of the samples from the Melamchi catchment in Nepal.

Sample	A68	A71	A69	A31
Natural water content (%)	9	9	8	32
Unit weight (g cm^{-3})	1.38	1.65	1.34	1.51
Dry density (g cm^{-3})	1.27	1.52	1.25	1.16
Liquid limit (%)	36	23	35	23
Cohesion (kPa)	12	7	14	14
Friction angle ($^{\circ}$)	27	29	30	32
Quartz (%)	57	36	59	64
Plagioclase (%)	19	11	16	15
Chlorite (%)	4	0	4	3
Muscovite (%)	4	20	4	3
Kaolinite (%)	4	5	3	3
Other minerals (%)	12	28	14	12

Table 2. Cutoff grain size and clay fraction (i.e., fraction smaller than 2 μm) of the tested samples.

Sample	Cutoff grain size (μm)	Clay fraction (%)
A68	125	12
	62	16
	20	17
A71	125	16
	62	21
	20	23
A69	125	12
	62	16
	20	21
A31	125	11
	62	14
	20	19

2.3 Methods

A Bromhead-type ring-shear device manufactured by Controls S.p.A. was used (Fig. 2). The device is equipped with computerised control of the normal load and rate of shearing and monitoring of the shearing resistance and vertical settlement. The annular box accommodating the material has an inner diameter of 70 mm, an outer diameter of 100 mm, and a height of 5 mm (Fig. 2). Drainage is ensured by two roughened porous brass platens placed at the top and bottom bases. Lateral confinement is provided by a stiff metal frame. The box rotates, powered by an electric motor able to provide a wide range of angular speeds. The top platen, screwed to a metal cap through which the normal load is applied, remains still as it is contrasted by two stiff load cells, installed with opposite orientations and both perpendicular to a stiff arm extending from the top cap. The box is placed in a bath of deionised water that is topped up periodically to prevent desaturation of the material. The device was modified to control the temperature of the water bath (Loche and Scaringi, 2023). Water from a 3 L thermostatic bath was circulated in a metal pipe, which was thermally insulated except for the portion immersed in the bath.

A thermocouple was installed in the proximity of the top porous platen, as close as possible to the material, to monitor the temperature during the experiments.

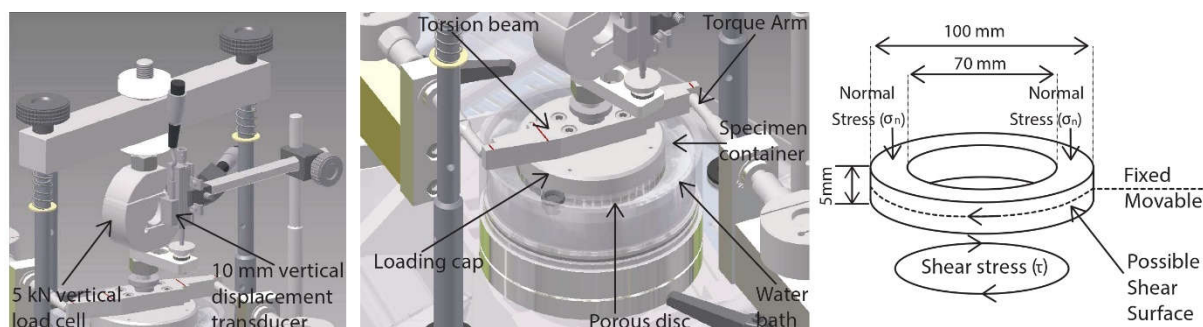


Figure 2. Schematics of the Bromhead-type ring-shear device used for the experiments with the indication of key elements and sample dimensions (mod. from Loche & Scaringi, 2023).

A thick paste was prepared by mixing the dry sieved material with deionised water to reach a water content less than the liquid limit in order to limit the settlement during consolidation. This was verified by repeatedly performing fall cone tests during sample preparation. However, no systematic measurement of the consistency index was made. Similarly, the water content and bulk density prior to the experiments were not measured as they are not expected to influence the shear behaviour of the soil once it reaches the residual shear condition.

After preparation, the paste was left to hydrate for at least 24 hours under a plastic cover so as to ensure full water saturation. It was then placed in the shear box, carefully filling gaps and removing air bubbles. Overconsolidation of the specimens was achieved by stepwise loading to 600 kPa and then unloading to 150, 100, or 50 kPa according to needs. Dissipation of the pore water pressure excess, not tracked directly, was ensured by monitoring the consolidation curve.

The specimens were then sheared at a rate of 0.1 mm/min until the residual shear condition was achieved. Further shearing for at least 10 mm was performed prior to increasing the temperature of the water bath from room temperature, 20 °C, to about 50 °C with the shearing ongoing. About 30 min elapsed from the beginning of heating until a steady value of temperature was recorded in the bath. To attain a steady state within the material and allow for the dissipation of any transient condition that may have arisen, such as thermal pressurisation, the temperature of the bath was kept elevated for up to 8 hours or until a steady value of shearing resistance could be evaluated. Finally, the thermostatic bath and circulation pump were turned off, and the system was allowed to cool down to room temperature. Meanwhile, the specimen was sheared further, and the shearing resistance after the heating-cooling cycle was recorded. In total, 36 experiments were conducted, exploring 3 values of normal stress \times 3 grain size cutoffs \times 4 samples.

3 Results

A representative result is shown in Fig. 3a, where the shearing resistance before, during, and after the phase at elevated temperature is plotted vs. the shearing distance for the 9 specimens obtained from sample A68 (3 normal stress values \times 3 grain-size cutoffs). Tests conducted with a larger cutoff size (lower clay fraction) did not show significant changes in steady-state resistance with temperature, while some weakening emerged for smaller cutoff sizes and larger normal stresses. The larger normal stress facilitates the formation of a shear zone with preferential particle orientation; this is conducive to lower resistance, as confirmed by the decrease in friction coefficient with the normal stress increasing. Particle alignment has a more pronounced effect on the shearing resistance of clay minerals, which, moreover, tend to exhibit lower friction than non-clay minerals. In fact, as the cutoff grain size decreases, the resistance decreases, and the dependence on the normal stress becomes more pronounced.

In Fig. 3a, a transient response to heating is shown in the form of a rapid increase in resistance, followed by a more gradual drop to the steady-state value. This could be explained by a rapid decrease in pore water pressure in (a portion of) the shear zone as a consequence of the rapid heating, which dissipates according to the soil's hydraulic conductivity. The phenomenon is not easy to interpret owing to the transient and non-uniform heating, which proceeds through the steel and brass elements as well as directly through the cell water in both radial and axial directions. Furthermore, the material is not homogeneous and has an anisotropic structure, with a softened top layer (the shear zone) and an overconsolidated underlying layer. In principle, this should not affect the residual shear strength but could play a role in the thermal response. In fact, the two layers should have different porosity and arrangements of the solid skeleton, with different thermal, mechanical, and hydraulic properties. In principle, a homogeneous soil sample undergoing rapid heating should exhibit a transient thermal pressurisation (and hence a decrease in shearing resistance) owing to positive pore water pressures arising from the larger thermal expansion of water compared to that of the mineral grains.

As for the steady-state response, the decrease in shearing resistance could be related to a decrease in water viscosity and/or to more efficient lubrication provided by the clay minerals against the larger and bulkier non-clay grains. Given the comparatively low clay fraction, even under the smallest cutoff size, it may be reasonable to hypothesise that grain-to-grain shearing of bulky particles mainly occurs, facilitated by the hydrated clay minerals, rather than clay-to-clay shearing. This is supported by the comparatively high value of friction coefficient in all tests (see also Fig. 3b), corresponding to friction angles around 25° , which are lower than typical friction angles of sands but are higher than residual friction angles attainable in clay-rich soils and gouges under the explored normal stress.

A summary of the effect of the clay fraction on the residual friction angle and the steady-state response to heating is provided in Fig. 4. Here, the friction angle is evaluated from the slope of the Mohr-Coulomb failure envelope calculated from the steady-state values of shearing resistance under the three normal stresses (50, 100, 150 kPa), assuming no cohesion intercept. The heterogeneity of the samples does not allow for a clear trend to be observed. However, an increase in the thermal effect (difference between the residual friction angle evaluated at 20°C and at 50°C) with the clay fraction can be intuited. This effect is, however, small (up to $\sim 1^\circ$ of friction angle or $\sim 4\%$ loss of resistance upon 30°C of heating) and may not be significant in the stability of slopes or kinematics of landslides, where the amplitude of thermal forcing is comparable to that applied in the experiments only close to the ground surface.

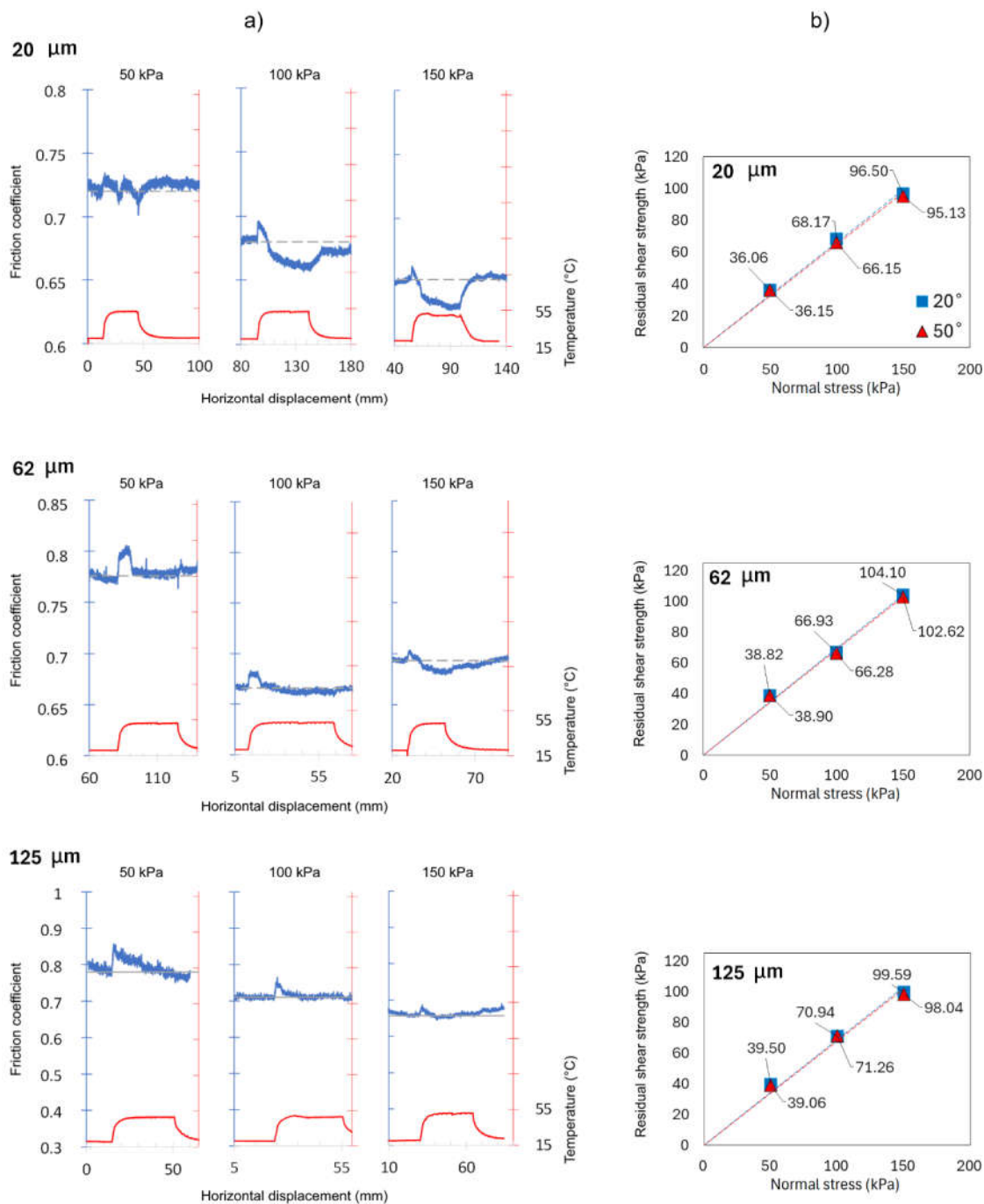


Figure 3. a) Frictional resistance (residual shear strength) and temperature (measured in the water bath) vs. shear displacement for one of the samples (A68). The experiments were conducted on specimens prepared at different cutoff grain sizes (20, 62, and 125 μm), sheared at a rate of 0.1 mm/min under normal stresses of 50, 100, and 150 kPa. b) Failure envelopes obtained from the experiments shown in a).

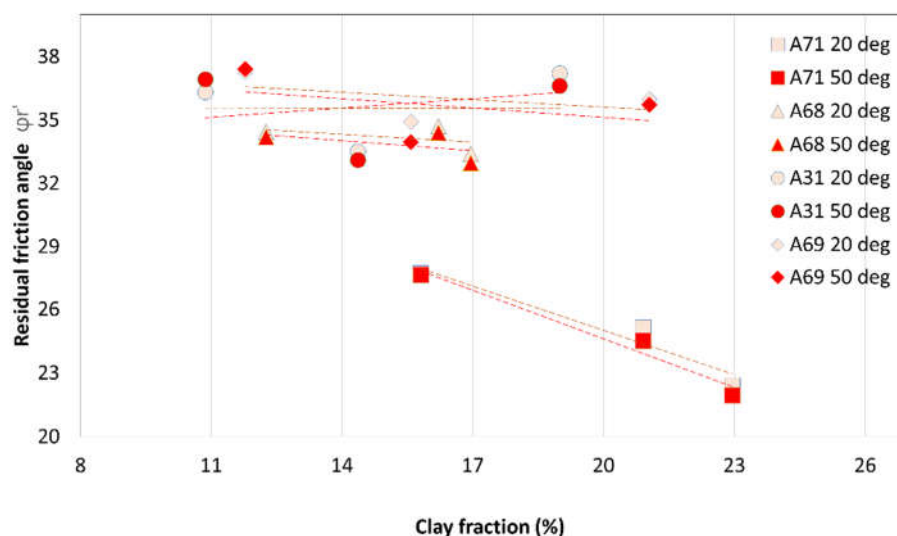


Figure 4. Residual friction angle as a function of clay fraction and temperature for the four samples investigated in this study. The values of residual friction angle were computed by linearly interpolating the results obtained under normal stresses of 50, 100, and 150 kPa for each sample and cutoff grain size, assuming no cohesion intercept. The coefficient of determination R^2 for all interpolations was >0.98 .

4 Conclusion

The purpose of this study was to evaluate how temperature affects the residual shear strength of natural landslide soils containing a small proportion of clay minerals. This study complements previous research that focused on pure clays or artificial mixtures and demonstrated that temperature may have a measurable effect on the residual shear strength for values of clay fraction of $\sim 10\%$ and above. Considering the low-plasticity nature of the clay minerals in the tested samples and, particularly, the likely absence of smectites, this threshold value may be smaller for the generality of soils. The magnitude of the effect was, however, small and unlikely to affect the global slope stability. Yet, the effect may be significant in the shallow portion of the ground, where seasonal and even daily thermal excursions can be large and may contribute to deformation phenomena in both soil covers and exposed rock. In future research, we will be using a larger number of natural samples from diverse landslide sites in order to explore the effects of clay fraction and clay minerals content on the thermal sensitivity of the residual shear strength without the need to rework the samples through successive sieving. This way, we aim to obtain charts that will be more representative of the natural variety of clay properties.

Acknowledgements

This research was supported by the Johannes Amos Comenius Programme (P JAC), project No. CZ.02.01.01/00/22_008/0004605, Natural and anthropogenic georisks. Support from the Czech Science Foundation (GAČR grant No. 24-12316S) and the Ministry of Education and Culture of the Czech Republic (MŠMT ERC CZ grant No. LL2316) are also acknowledged. O. Dhakal acknowledges support from the Charles University Grant Agency (GAUK grant No. 68624).

References

Badakhshan, E., Vaunat, J., Veylon, G., 2024. Meteorological and vegetation effects on the thermal analysis of slopes. *Renewable and Sustainable Energy Reviews* 196, 114352. <https://doi.org/10.1016/j.rser.2024.114352>

- Dhital, M.R., 2015. *Geology of the Nepal Himalaya: Regional Perspective of the Classic Collided Orogen*. Springer.
- Di Maio, C., 1996. Exposure of bentonite to salt solution: osmotic and mechanical effects. *Géotechnique* 46, 695–707. <https://doi.org/10.1680/geot.1996.46.4.695>
- Di Maio, C., Scaringi, G., 2016. Shear displacements induced by decrease in pore solution concentration on a pre-existing slip surface. *Engineering Geology* 200, 1–9. <https://doi.org/10.1016/j.enggeo.2015.11.007>
- Di Maio, C., Scaringi, G., Vassallo, R., 2015. Residual strength and creep behaviour on the slip surface of specimens of a landslide in marine origin clay shales: influence of pore fluid composition. *Landslides* 12, 657–667. <https://doi.org/10.1007/s10346-014-0511-z>
- Duque, J., Loche, M., Scaringi, G., 2023. Rate-dependency of residual shear strength of soils: implications for landslide evolution. *Géotechnique Letters* 13, 1–8. <https://doi.org/10.1680/jgele.23.00004>
- Garcia, L.M., Pinyol, N.M., Lloret, A., Soncco, E.A., 2023. Influence of temperature on residual strength of clayey soils. *Engineering Geology* 323, 107220. <https://doi.org/10.1016/j.enggeo.2023.107220>
- Goren, L., Aharonov, E., 2007. Long runout landslides: The role of frictional heating and hydraulic diffusivity. *Geophysical Research Letters* 34. <https://doi.org/10.1029/2006GL028895>
- Guglielmi, S., Pirone, M., Dias, A.S., Cotecchia, F., Urciuoli, G., 2023. Thermohydraulic Numerical Modeling of Slope-Vegetation-Atmosphere Interaction: Case Study of the Pyroclastic Slope Cover at Monte Faito, Italy. *Journal of Geotechnical and Geoenvironmental Engineering* 149, 05023005. <https://doi.org/10.1061/JGGEFK.GTENG-11240>
- Hu, W., Scaringi, G., Xu, Q., Van Asch, T.W.J., Huang, R., Han, W., 2018. Suction and rate-dependent behaviour of a shear-zone soil from a landslide in a gently-inclined mudstone-sandstone sequence in the Sichuan basin, China. *Engineering Geology* 237, 1–11. <https://doi.org/10.1016/j.enggeo.2018.02.005>
- Kohler, M., Hottiger, S., Puzrin, A.M., 2023. Rate, Water Pressure, and Temperature Effects in Landslide Shear Zones. *Journal of Geophysical Research: Earth Surface* 128, e2023JF007220. <https://doi.org/10.1029/2023JF007220>
- Loche, M., Scaringi, G., 2023. Temperature and shear-rate effects in two pure clays: Possible implications for clay landslides. *Results in Engineering* 20, 101647. <https://doi.org/10.1016/j.rineng.2023.101647>
- Massey, C.I., Petley, D.N., McSaveney, M.J., Archibald, G., 2016. Basal sliding and plastic deformation of a slow, reactivated landslide in New Zealand. *Engineering Geology* 208, 11–28. <https://doi.org/10.1016/j.enggeo.2016.04.016>
- Mesri, G., Olson, R.E., 1970. Shear Strength of Montmorillonite. *Géotechnique* 20, 261–270. <https://doi.org/10.1680/geot.1970.20.3.261>
- Mitchell, J.K., 1991. Conduction phenomena: from theory to geotechnical practice. *Geotechnique* 41, 299–340.
- Scaringi, G., Di Maio, C., 2016. Influence of Displacement Rate on Residual Shear Strength of Clays. *Procedia Earth and Planetary Science* 16, 137–145. <https://doi.org/10.1016/j.proeps.2016.10.015>
- Scaringi, G., Hu, W., Xu, Q., Huang, R., 2018. Shear-Rate-Dependent Behavior of Clayey Bimaterial Interfaces at Landslide Stress Levels. *Geophysical Research Letters* 45, 766–777. <https://doi.org/10.1002/2017GL076214>
- Scaringi, G., Loche, M., 2024. Temperature and Rate Effects on the Residual Shear Strength of Clays: A State of the Art, in: *Proceedings of the 6th Regional Symposium on Landslides in the Adriatic-Balkan Region, ReSyLAB2024* (Eds. Marjanović and Đurić). Belgrade (Serbia), pp. 247–251.

- Scaringi, G., Loche, M., 2022. A thermo-hydro-mechanical approach to soil slope stability under climate change. *Geomorphology* 401, 108108. <https://doi.org/10.1016/j.geomorph.2022.108108>
- Shibasaki, T., Matsuura, S., Hasegawa, Y., 2017. Temperature-dependent residual shear strength characteristics of smectite-bearing landslide soils: Temperature-Dependent Residual Strength. *Journal of Geophysical Research: Solid Earth* 122, 1449–1469. <https://doi.org/10.1002/2016JB013241>
- Shibasaki, T., Matsuura, S., Okamoto, T., 2016. Experimental evidence for shallow, slow-moving landslides activated by a decrease in ground temperature: Landslides Affected by Ground Temperature. *Geophysical Research Letters* 43, 6975–6984. <https://doi.org/10.1002/2016GL069604>
- Shrestha, S., Shrestha, M., Babel, Mukand.S., 2016. Modelling the potential impacts of climate change on hydrology and water resources in the Indrawati River Basin, Nepal. *Environ Earth Sci* 75, 280. <https://doi.org/10.1007/s12665-015-5150-8>
- Skempton, A.W., 1985. Residual strength of clays in landslides, folded strata and the laboratory. *Geotechnique* 35, 3–18.
- Skempton, A.W., 1964. Long-term stability of clay slopes. *Geotechnique* 14, 77–102.
- Tika, T.E., Vaughan, P.R., Lemos, L.J.L.J., 1996. Fast shearing of pre-existing shear zones in soil. *Géotechnique* 46, 197–233. <https://doi.org/10.1680/geot.1996.46.2.197>